# Origin of Graphitic Carbon and Pentlandite in Matrix Olivines in the Allende Meteorite

**Adrian J. Brearley**

Matrix olivines in the Allende carbonaceous chondrite are believed to have formed by condensation processes in the primitive solar nebula. However, transmission electron microscope observations of numerous matrix olivines show that they contain abundant, previously unrecognized, nanometer-sized inclusions of pentlandite and poorly graphitized carbon. Neither of these phases would have been stable at the high-temperature conditions required to condense iron-rich olivine in the solar nebula. The presence of these inclusions is consistent with formation of the olivines by parent body processes that involved overgrowth of fine-grained organic materials and sulfides in the precursor matrix materials.

Carbonaceous chondrites are a primitive group of meteorites that formed 4.56 billion years ago within the solar nebula, a dynamic, disk-shaped region of dust and gas with the protosun at its center (*1*). Carbonaceous chondrites contain a number of diverse components, including chondrules, calcium-aluminum–rich inclusions (CAI), matrix, and organic compounds. Each of these components provides information about the composition, pressure, temperature, and lifetime of the solar nebula. The origin of the carbonaceous material in these meteorites, in particular, has received considerable attention because many of the compounds present are the building blocks of life. An understanding of the spatial distribution of organic matter in chondritic meteorites can help to explain the origin of this material, its distribution in interstellar or nebular dust, and how it was processed in meteorite parent bodies. Here I present in situ observations of carbonaceous material in matrix olivines in the Allende CV3 carbonaceous chondrite that are consistent with a complex parent body history for this meteorite.

The bulk of the organic carbon in carbonaceous chondrites is a macromolecular material containing H, N, O, and S (*2*). However, the Allende meteorite contains an extremely low abundance of this material: Of the 0.25 weight % carbon in Allende (*3*), most appears to be elemental carbon (*2*). Transmission electron microscope (TEM) studies (*4*) of Allende acid residues have shown that the dominant carbon form present consists of fine-grained ($<0.1$ μm), poorly graphitized carbon (PGC) that occurs as tangled crystallites of a few unit cells in thickness.

The matrix of Allende consists mainly of platy FeO-rich ($Fa_{38-56}$) olivine (*5–7*) with a range of grain sizes ($<3$ to 20 μm). Smaller ($<3$ μm), subrounded olivine grains occur interstitially to the larger olivine grains (*7*). Several minor phases occur, including nepheline, Ca-rich clinopyroxene, pentlandite [$(Fe,Ni)_9S_8$], and awaruite ($Ni_3Fe$) (*6*). In this study, numerous ($\sim$100) matrix olivine grains from several different regions of a thin section of Allende were examined in detail by TEM (*8*). Many more grains ($\sim$200 to 300) with the same microstructural features described below were observed but were not studied in detail. The olivines all contain abundant submicrometer inclusions and numerous features that appear to be voids (Fig. 1A), microstructures that have been noted previously (*9*) but not described in detail. High-resolution TEM (HRTEM) studies, x-ray microanalysis, and electron diffraction show that the dominant inclusion phase is pentlandite (Fig. 1B), with grain sizes $<50$ nm. The pentlandite grains are distributed randomly within the olivine grains, and their abundance varies from one olivine grain to another. The pentlandites are not crystallographically oriented with respect to the host olivine. Most pentlandite grains are rounded to subrounded in shape, but some grains have well-developed facets (Fig. 1B). HRTEM of pentlandite grains shows that they are always associated with fine-grained crystals of PGC (*10*) (Fig. 1B). The PGC typically occurs as small, isolated crystallites, a few nanometers in length, along the interface between the pentlandite and enclosing olivine. It can also occur as continuous rims around individual grains. HRTEM studies of the voidlike features show that they are partially to completely filled by PGC crystallites a few unit cells in thickness (Fig. 1C) and pentlandite is absent. Some voids are lined by rims of PGC that is associated with amorphous carbon (Fig. 1D).

The origin of matrix olivines in Allende is controversial (*11*). Formation by condensation from a cooling solar nebular gas has been widely accepted as the most plausible origin for these olivines (*12*, *13*). However, this origin requires condensation under more oxidizing conditions than that of a gas of solar composition, in regions of the nebula where the dust-to-gas ratio is enhanced (*12*). Under such conditions, calculated condensation temperatures of FeO-rich olivine are 1200 K at a gas pressure of $10^{-6}$ bars or 1400 K at $10^{-3}$ bars (*12*).

The presence of PGC and pentlandite inclusions within Allende matrix olivines is not consistent with this model. During condensation from a cooling nebular gas, troilite (FeS), rather than pentlandite, is the stable sulfide phase that forms at temperatures $<710$ K, by reaction of Fe metal with $H_2S$ (*14*), although pentlandite, instead of troilite, can form during this reaction if the metal is Ni-bearing (*15*). Pentlandite is only stable at temperatures $<883$ K (*16*) and hence would not be a stable phase in the nebula at the conditions required to condense FeO-rich olivine.

This conclusion is supported by consideration of the origin of the PGC inclusions. PGC is formed by the thermal processing of graphitizeable carbons (*17*) that are typically complex, macromolecular organic compounds such as kerogens (*18*). Graphitization is a thermally activated, irreversible thermodynamic process that is sluggish and involves the progressive loss of H, N, and O from the organic material. This process results in the progressive formation of ordered domains with the two-dimensional structure of nongraphitic carbons (*17*, *19*). Crystalline graphite is formed when this process has gone to completion (*17*). In terrestrial metamorphic rocks, graphitization occurs between $\sim$200° and $-500$°C (*20*), and the PGC passes through a range of degrees of ordering. Within a nebular environment, the macromolecular material, which is the precursor to PGC, forms at low temperatures because above $\sim$600 K at $10^{-5}$ atm, CO is the stable carbon compound at solar C/O ratios ($\sim$0.6) (*21*). At temperatures below $\sim$400 K, organic molecules can form by several different mechanisms (*21*). Thus, if the FeO-rich olivines were produced by condensation under oxidizing conditions, temperatures would have been too high to stabilize complex organic molecules. Hence, they would not have been available to be incorporated into the condensate olivine.

An alternative scenario is that the olivines were produced by evaporation of preexisting carbon-bearing dust, which then recondensed. In this case, the inclusions of carbonaceous material would represent material that survived the evaporation event and was captured within the olivine grains. However, it seems implausible that carbonaceous material would survive in the high-temperature oxidizing environment required to form FeO-rich olivine, because stepwise combustion experiments show that the bulk of Allende

Department of Earth and Planetary Sciences, University of New Mexico, Albuquerque, NM 87131, USA. E-mail: brearley@unm.edu

carbon decomposes below 973 K (*22*). Pentlandite would certainly not have survived either. Furthermore, during condensation, more common refractory minerals, such as forsteritic olivines and pyroxenes, should be captured by the olivine grains, but none have been found as inclusions. Such phases would certainly have been present in nebular dust (*6*, *23*). There does not appear to be a viable mechanism for concentrating carbon in olivine grains during condensation while excluding more common nebular phases.

Alternatively, it has been proposed that FeO-rich matrix olivines in Allende (*24–26*) formed by a complex sequence of parent body processes involving an episode of aqueous alteration followed by metamorphism. This aqueous alteration event is recorded in chondrules by the presence of hydrous phases that have replaced enstatite (*27*). On the basis of the upper thermal stabilities of the hydrous phases present, the metamorphic event took place at temperatures <400°C (*27*). In this scenario, the FeO-rich olivines formed by dehydration of phases such as Fe serpentines, with compositions similar to those found in CM carbonaceous chondrites (*28*). This model provides a plausible explanation for the characteristics of matrix olivines in Allende. Insoluble macromolecular carbon constitutes ~70% of the organic carbon in CM carbonaceous chondrites (*2*) and was probably the precursor of the PGC in Allende. In chondrites with hydrated matrices, this material is probably intimately mixed with phyllosilicate phases. If matrix olivines in Allende formed by dehydration of hydrous phases, then they would have overgrown grains of carbonaceous material as they developed, forming inclusions, because this macromolecular component cannot be incorporated into the growing olivine. Graphitization of the macromolecular carbon probably occurred during the metamorphic event.

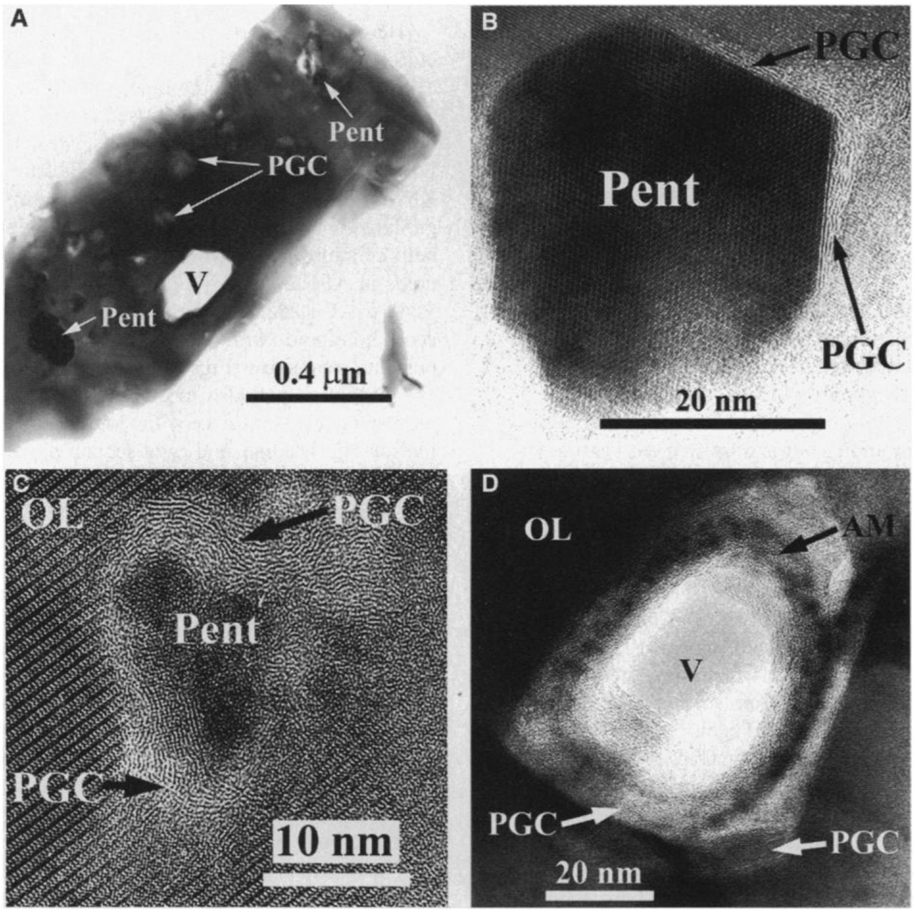


**Fig. 1.** Transmission electron micrographs of Allende matrix olivines. (**A**) Electron micrograph of a typical platy matrix olivine. The olivine contains numerous voids (V) and inclusions of pentlandite (Pent) and graphitic material (PGC). (**B**) HRTEM image of a faceted pentlandite inclusion within a matrix olivine. The pentlandite is partly rimmed by a thin layer of PGC, with a relatively high degree of order indicated by the wavy, continuous (002) lattice fringes. (**C**) HRTEM image of an inclusion of PGC and pentlandite within a matrix olivine (OL). The PGC has a high degree of disorder indicated by the short, subparallel, wavy (002) lattice fringes with basal spacings ranging from 0.35 to 0.39 nm. The central part of the inclusions consists of three nanometer-sized pentlandite grains. (**D**) HRTEM image of a carbonaceous inclusion in a matrix olivine (OL). The central part of the inclusions is a hole (V) that is surrounded by a region of amorphous carbon and finally a layer of PGC immediately adjacent to the olivine host. The PGC lines the whole inclusion.

Pentlandite inclusions in the olivine can be explained by the dehydration of Ni- and S-bearing Fe-enriched serpentines (*28*). Neither Ni or S is readily accommodated into the olivine structure and will be released to form pentlandite when the serpentine dehydrates. The presence of voids within the olivine is also consistent with such an origin. In Yamato 82162, a thermally metamorphosed carbonaceous chondrite, olivine grains formed by dehydration of hydrous phases contain numerous voids analogous to those in Allende matrix olivines (*29*). Observations on Yamato 793321 (*30*) also show that the breakdown of serpentine grains to produce olivines results in grains with platy, elongate morphologies that are similar to those of Allende matrix olivines.

One objection to this model is that the oxygen isotopic composition of Allende matrix lies exactly on the carbonaceous chondrite anhydrous mineral (CCAM) mixing line (slope = 0.94) in a three-isotope oxygen plot (*11*, *31*). The CCAM was believed to represent the primitive oxygen isotopic composition of components in Allende; any parent body alteration of Allende matrix would have displaced its isotopic composition from this line (*31*). However, recent high spatial resolution oxygen isotopic data for CAIs in Allende (*32*) indicate that the primitive oxygen isotopic composition of components in Allende actually lies along a line with slope of exactly 1. Therefore, the CCAM line probably represents an artifact produced by mixing of a primitive oxygen reservoir with a fractionated component near the terrestrial fractionation line. Matrix does not, therefore, have a primitive oxygen isotopic composition, and its displacement from the slope = 1 line is consistent with parent body alteration. Furthermore, the composition of matrix lies along a mass-dependent fractionation line of slope = one-half, defined by altered regions of CAIs and chondrules (*32*, *33*), that is most readily explained by interaction with an aqueous fluid in a parent body environment.

### References and Notes

1. P. Cassen, in *Chondrules and the Protoplanetary Disk*, R. H. Hewins, R. H. Jones, E. R. D. Scott, Ed. (Cambridge Univ. Press, Cambridge, 1996), pp. 21–28.
2. J. R. Cronin, S. Pizzarello, D. P. Cruikshank, in *Meteorites and the Early Solar System*, J. F. Kerridge and M. S. Matthews, Eds. (Univ. of Arizona Press, Tucson, AZ, 1988), pp. 819–857.
3. E. Jarosewich, R. S. J. Clarke, J. N. Barrows, *Smithson. Contrib. Earth Sci.* **27**, 1 (1987).
4. P. P. K. Smith and P. R. Buseck, *Science* **212**, 322 (1981).
5. H. W. Green, S. V. Radcliffe, A. H. Heuer, *ibid.* **172**, 936 (1971).
6. E. R. D. Scott, D. J. Barber, C. M. O. Alexander, R. Hutchison, J. A. Peck, in *Meteorites and the Early Solar System*, J. F. Kerridge and M. S. Matthews, Ed. (Univ. of Arizona Press, Tucson, AZ, 1988), pp. 718–745.
7. M. Toriumi, *Earth Planet. Sci. Lett.* **92**, 265 (1989).
8. Doubly polished thin sections of Allende, mounted with Loctite 414 epoxy, were prepared. Regions of the matrix were characterized by scanning electron microscopy

and electron microprobe analysis. Slotted copper grids were glued over areas of interest, and the samples were removed by immersion in acetone. Samples were prepared for TEM by ion-beam milling, with a Gatan ion-beam mill. TEM was carried out on a JEOL 2010 HRTEM, operating at 200 kV. A Link ISIS energy-dispersive x-ray analysis system, equipped with a Link Pentafet ultrathin window energy-dispersive spectrometer, was used to obtain in situ mineral analyses with the Cliff-Lorimer thin film approximation for data reduction. Experimental k factors were used throughout.

9. J. R. Ashworth and D. J. Barber, *Earth Planet. Sci. Lett.* **27**, 43 (1975).
10. PGC has a crystal structure intermediate between that of well-crystallized graphite, which has a three-dimensional crystal structure, and the two-dimensional structure of nongraphitic carbons. PGC consists of crystallites of carbon that have a fraction of their layers oriented as in graphite, with the remaining layers in random orientations [R. E. Franklin, *Acta Crystallogr.* **4**, 253 (1951)]. PGC was identified with high-resolution lattice imaging, electron diffraction techniques, and morphology. Lattice spacings were measured either directly from HRTEM images or from electron diffraction patterns produced by fast Fourier transform of digital HRTEM images.
11. M. K. Weisberg and M. Prinz, *Meteoritics Planet. Sci.* **33**, 1087 (1998).
12. H. Palme and B. Fegley Jr., *Earth Planet. Sci. Lett.* **101**, 180 (1990).
13. G. J. MacPherson, A. Hashimoto, L. Grossman, *Geochim. Cosmochim. Acta* **49**, 2267 (1985).
14. J. W. Larimer and E. Anders *ibid.* **31**, 1239 (1967).
15. D. S. Lauretta, K. Lodders, B. Fegley Jr., *Meteoritics Planet. Sci.* **33**, 821 (1998).
16. G. Kullerud, *Carnegie Inst. Yearb.* **62**, 175 (1963).
17. D. B. Fischbach, in *Physics and Chemistry of Carbon*, P. L. Walker, Ed. (Dekker, New York, 1971), vol. 7, pp. 1–105.
18. B. Durand, *Kerogens* (Editions Technip, Paris, 1980).
19. P. R. Buseck, B.-J. Huang, B. Miner, *Org. Geochem.* **12**, 221 (1988).
20. A. J. Brearley, *Geochim. Cosmochim. Acta* **54**, 831 (1990).
21. R. Hyatsu, R. G. Scott, M. H. Studier, R. S. Lewis, E. Anders, *Science* **208**, 1515 (1980).
22. P. K. Swart, M. M. Grady, I. P. Wright, C. T. Pillinger, *Proc. Lunar. Planet. Sci. Conf. 13th*, *J. Geophys. Res.* **87** (suppl.), A283 (1982).
23. A. J. Brearley, in *Chondrules and the Protoplanetary Disk*, R. H. Hewins, R. H. Jones, E. R. D. Scott, Eds. (Cambridge Univ. Press, Cambridge, 1996), pp. 137–152.
24. T. Kojima and K. Tomeoka, *Meteoritics* **30**, 529 (1995).
25. A. N. Krot, E. R. D. Scott, M. E. Zolensky, *ibid.*, p. 748.
26. ———, *ibid.* **32**, 31 (1997).
27. A. J. Brearley, *Science* **276**, 1103 (1997).
28. T. E. Bunch and S. Chang, *Geochim. Cosmochim. Acta* **44**, 1543 (1980).
29. J. Akai, *Proc. Natl. Inst. Polar Res. Symp. Antarct. Meteorites* **7**, 94 (1994).
30. ———, *Geochim. Cosmochim. Acta* **52**, 1593 (1988).
31. R. N. Clayton, in *Workshop on Parent-Body and Nebular Modification of Chondritic Materials*, M. E. Zolensky, A. N. Krot, E. R. D. Scott, Eds. (LPI Technical Report No. 97-02, Lunar and Planetary Institute, Houston, TX, 1997), pp. 10–11.
32. E. Young and S. S. Russell, *Science* **282**, 452 (1998).
33. R. D. Ash, E. D. Young, C. M. O. D. Alexander, D. Rumble III, G. J. MacPherson, *Lunar Planet. Sci.* **XXX** (abstract 1836) (1999) [CD-ROM].
34. This research was supported by NASA grant NAGW-3347 to J. J. Papike. Electron microscopy was performed in the Electron Microbeam Analysis Facility, Department of Earth and Planetary Sciences and Institute of Meteoritics, University of New Mexico.

9 June 1999; accepted 21 July 1999

# *Equatorius*: A New Hominoid Genus from the Middle Miocene of Kenya

**Steve Ward,[1] Barbara Brown,[2] Andrew Hill,[3] Jay Kelley,[4] Will Downs[5]**

**A partial hominoid skeleton just older than 15 million years from sediments in the Tugen Hills of north central Kenya mandates a revision of the hominoid genus *Kenyapithecus*, a possible early member of the great ape–human clade. The Tugen Hills specimen represents a new genus, which also incorporates all material previously referable to *Kenyapithecus africanus*. The new taxon is derived with respect to earlier Miocene hominoids but is primitive with respect to the younger species *Kenyapithecus wickeri* and therefore is a late member of the stem hominoid radiation in the East African Miocene.**

An important issue in hominoid systematics concerns the origin of the great ape and human clade. Estimated divergence times among the lineages of extant great apes and humans based on comparative genetics suggest that the last common ancestor of this clade may have lived during the Middle Miocene (about 16 to 11 million years ago) (*1*). The African Middle Miocene hominoid *Kenyapithecus* has been considered to be either an early member of the clade or its sister taxon (*2–4*). Most recent analyses, however, consider *Kenyapithecus* to be too primitive to be closely related to extant great apes and humans (*1, 5–7*).

Two species of *Kenyapithecus* are currently recognized: *K. wickeri*, from the type locality at Fort Ternan in western Kenya, and *K. africanus*, from several localities in western Kenya, the Tugen Hills, and Nachola in the Samburu region (Fig. 1). All sites producing fossils referable to the genus range in age between 15.5 and ~14 million years ago. The fossils from Fort Ternan, at ~14 million years, are younger in age than all known *K. africanus* specimens. The genus *Kenyapithecus* has been controversial since its initial diagnosis (*8*), in part because of the small sample of *K. wickeri* specimens but also because of a paucity until recently of similarly aged large hominoid fossils from Africa and elsewhere. Consequently, the congeneric status of *K. wickeri* and *K. africanus*, as well as hypotheses that place either of these taxa in the ancestry of modern apes and humans have been questioned (*1, 5–7, 9–14*).

Here we describe a partial hominoid skeleton from locality BPRP 122 at Kipsaramon, a Middle Miocene site complex in the Muruyur Formation that is exposed along the northern crest of the Tugen Hills, west of Lake Baringo in central Kenya. The skeleton, KNM-TH 28860, provides new evidence regarding the taxonomic diversity and phylogenetic relationships of Middle Miocene hominoids in Africa.

KNM-TH 28860 is the first Middle Miocene hominoid with associated teeth and postcranial remains (Figs. 2 and 3; Table 1). The specimen includes most of a mandible preserving all teeth except the right central incisor, right canine, and right second molar. Also included are the left maxillary central incisor and both lateral incisors. Postcranial elements include portions of the scapula and sternum, a clavicle, numerous rib fragments, most of the right humerus and the head of the left humerus, a complete right radius, half of the right ulna and parts of the left ulna and radius, five carpal bones, and portions of several fingers. Also preserved are one complete lower thoracic vertebra and other fragmentary thoracic vertebrae. Regressions of dental and long bone dimensions on body mass in a variety of extant primates (*15*) suggest a body mass of approximately 27 kg.

The maxillary central incisor crown is relatively broad mesiodistally in proportion to its height (Fig. 2). There is a low but distinct basal lingual tubercle and a distinct, continuous lingual cingulum on the mesial, distal, and basal margins. The $I^2$ crown is highly asymmetrical, with a lingual cingulum that "spirals" apically from the mesial to the distal margins of the crown (Fig. 2). The mandibular canine is low-crowned relative to basal crown dimensions, and its size and morphology indicate that KNM-TH 28860

[1]Department of Anatomy, Northeastern Ohio Universities College of Medicine, Post Office Box 95, Rootstown, OH 44272, USA, and Division of Biomedical Sciences, Kent State University, Kent, OH 44242, USA. [2]Department of Orthopaedic Surgery, Northeastern Ohio Universities College of Medicine, Rootstown, OH 44272, USA. [3]Department of Anthropology, Yale University, New Haven, CT 06520, USA. [4]Department of Oral Biology, College of Dentistry, University of Illinois at Chicago, Chicago, IL 60612, USA. [5]Bilby Research Center, Northern Arizona University, Flagstaff, AZ 86011, USA.